



Diversity of intraseasonal oscillation over the western North Pacific

Hui Wang¹ · Fei Liu^{1,2} · Bin Wang³ · Guosen Chen⁴ · Wenjie Dong¹

Received: 16 September 2020 / Accepted: 19 April 2021

© The Author(s), under exclusive licence to Springer-Verlag GmbH Germany, part of Springer Nature 2021

Abstract

The western North Pacific (WNP) intraseasonal oscillation (ISO) is the strongest over the globe, its prediction is the cornerstone for subseasonal prediction of the Asian summer monsoon. Yet, our understanding of the diversity of the WNP ISO is limited, which challenges our modeling and prediction efforts. We study the diversity of observed WNP ISO by performing cluster analysis on propagation patterns of ISO events, targeting three clusters: westward, northeastward, and northwestward propagations. The westward cluster exists within the WNP, while the other two are related to the northeastward propagating rain band originated from the central equatorial Indian Ocean and to the northwestward propagating dipole across the western Pacific and Indian Ocean, respectively. Moist static energy (MSE) tendency contributing to these different propagations is mainly due to horizontal advection, while radiative heating mainly maintains the ISO's development. Background sea surface temperature (SST) and MSE anomalies partly determine this ISO diversity, especially for those ISOs with large similarity. The westward cluster is related to warm SST anomalies in the western Indian Ocean, as a combination of seasonal cycle and internal interannual-to-interdecadal variability. The northeastward cluster is related to the cold Pacific Meridional Mode and La Niña-like pattern, while the northwestward cluster is related to the opposite warm background, both as the internal variability. Our finding of the background-affected ISO diversity over the WNP can be conducive to both model simulation and subseasonal prediction of the Asian summer monsoon.

Keywords Intraseasonal oscillation · Western North Pacific · Diversity · La Niña · Pacific Meridional Mode · Western Indian Ocean

1 Introduction

The intraseasonal oscillation (ISO) is the cornerstone of subseasonal prediction of the Asian summer monsoon (Wang et al. 2009; Lau et al. 2012). The strongest ISO of the globe appears over the western North Pacific (WNP) during the boreal summer, especially during late summer (Li and Wang 2005; Liu and Wang 2013). The ISO over the WNP not only impacts the South China Sea (SCS) summer monsoon onset (Zhou and Chan 2005; Lee et al. 2013; Shao et al. 2014; Wang et al. 2018), sub-seasonal sea surface temperature (SST) variability and the zonal oscillation of the western Pacific subtropical high (Ren et al. 2013), but also influences the East Asian summer monsoon through exciting an East Asian/Pacific pattern (Huang and Sun 1992) or Pacific-Japan (Nitta 1987)-like teleconnection (Guan et al. 2019; Sun et al. 2019b; Li et al. 2020; Liu et al. 2020). Synoptic-scale variabilities in the region, such as tropical cyclones over the WNP (Maloney and Hartmann 2000; Zhou and Li 2010; Li and Zhou 2013;

✉ Fei Liu
liufei26@mail.sysu.edu.cn

✉ Wenjie Dong
dongwj3@mail.sysu.edu.cn

¹ Key Laboratory of Tropical Atmosphere-Ocean System, Ministry of Education, Southern Marine Science and Engineering Guangdong Laboratory, School of Atmospheric Sciences, Sun Yat-Sen University, Zhuhai 519082, China

² State Key Laboratory of Numerical Modeling for Atmospheric Sciences and Geophysical Fluid Dynamics, Institute of Atmospheric Physics, Chinese Academy of Sciences, Beijing 100029, China

³ Department of Atmospheric Sciences, International Pacific Research Center, University of Hawaii at Manoa, Honolulu, HI 96822, USA

⁴ Earth System Modeling Center and Climate Dynamics Research Center, Nanjing University of Information Science and Technology, Nanjing 210044, China

Zhao et al. 2015) and extreme rainfall and heatwave events over the Asian summer monsoon region (Chen et al. 2016; Hsu et al. 2016, 2017), are also modulated by the ISO over the WNP. Understanding the ISO over the WNP is essential for improving the subseasonal prediction of tropical cyclone activity and Asian summer monsoon.

Our current numerical models still face huge challenges in their capability to model the ISO over the WNP (Lee et al. 2015; Neena et al. 2016; Jie et al. 2017). One reason lies in the complexity of the ISO propagation over the WNP. Different from the zonal propagation of the boreal-winter Madden Julian Oscillation (MJO), which shows diversified propagations in terms of fast eastward propagation, slow eastward propagation, standing, and jumping (Wang et al. 2019a), the boreal-summer ISO has northeastward propagation over the Indian Ocean (Yasunari 1979; Annamalai and Sperber 2005; Liu et al. 2016), and has northwestward propagation over the western Pacific (Murakami 1984; Lau and Chan 1986; Nitta 1987; Chen and Murakami 1988; Wang and Rui 1990; Hsu and Weng 2001; Kemball-Cook and Wang 2001). The ISO over the WNP also shows westward propagation (Murakami 1980; Wang and Rui 1990; Chen and Chen 1995; Kikuchi and Wang 2009) and even southward propagation (Liu et al. 2002; Lau et al. 2012). These complicated propagations of the boreal-summer ISO can also be observed by using the Multiple Object Tracking method as in Singh and Kinter (2020), though their work focused on the tropical ISO in all seasons. The diversity of the ISO over the Indian Ocean was studied by Pillai and Sahai (2015), which classified the ISO propagation into three types: eastward only, northward only, and northeastward propagations. The diversity of the WNP ISO, which is the strongest over the globe during late summer, however, has not been studied systematically.

In addition, the change of mean state has been found to determine the ISO change over the WNP, mainly on the interannual time scale (Liu et al. 2016; Wu and Cao 2017). The higher-frequency northwestward propagating ISO with a period shorter than 30 days was found to be intensified over the WNP during a central-to-eastern Pacific warming summer associated with the El Niño developing phase, with contributions from both easterly vertical shear anomaly and enhanced background moisture (Teng and Wang 2003; Deng and Li 2016; Liu et al. 2016; Wu and Cao 2017). The lower-frequency northeastward propagation with a period longer than 40 days, however, has been observed during a cold summer related to the La Niña decaying phase, because of enhanced background moisture over the Maritime Continent (MC) (Liu et al. 2016; Wu and Cao 2017). The southward propagation of the ISO originated from extratropical is only active in early summer, and the northward propagation dominates in late summer, which is related to the northward penetration of the East Asian summer monsoon (Tao and Chen 1987; Linho and Wang 2002; Lau et al. 2012).

Whether the ISO originated from the Indian Ocean can reach the western Pacific is determined by the mean state over the MC. The MC topography tends to block the eastward propagation of the ISO (Zhang and Ling 2017; Burleyson et al. 2018), limiting heat flux (Maloney and Sobel 2004; Sobel et al. 2008) and moist static energy (MSE) generation (Raymond 2001; Adames and Kim 2016) and consuming energy via diurnal cycle (Hagos et al. 2016; Sun et al. 2019a). The eastward MSE gradient should favor the ISO passing over the MC (Fu et al. 2017; Jiang 2017). Therefore, a systematic exploration of the underlying mechanism for the ISO diversity over the WNP is much needed.

To deepen our understanding of the ISO over the WNP and to improve subseasonal prediction of local extreme weather and Asian summer monsoon, we objectively detect the diversity of the ISO over the WNP and explore their underlying mechanisms. The paper is organized as follows. In Sect. 2, we introduce the data and method used in this study. In Sect. 3, we present the dominant mode of the ISO over the WNP. The diversity of the WNP ISO is discussed in Sect. 4. Different backgrounds that affect the diversity are discussed in Sect. 5, and our findings are summarized in Sect. 6.

2 Data and methods

To represent the convection of the ISO, we use daily-mean Advanced Very High-Resolution Radiometer (AVHRR) interpolated outgoing longwave radiation (OLR) data from the National Oceanic and Atmospheric Administration (NOAA) satellite (Liebmann 1996). This dataset has been used for both boreal-winter MJO and boreal-summer ISO (Wheeler and Hendon 2004; Lee et al. 2013). We also use daily SST, horizontal wind, air temperature, pressure velocity, specific humidity, geopotential height from 1000 to 100 hPa, surface latent and sensible heat fluxes, and net thermal and solar radiation from the European Centre for Medium Range Weather Forecasts (ECMWF) reanalysis-interim (ERA-interim) data (Dee et al. 2011). The horizontal resolution for these data is $2.5^\circ \times 2.5^\circ$. Daily averaged precipitation of the 3B42 version 7 of the Tropical Rainfall Measurement Mission (TRMM) during the period 1998–2018 (Huffman et al. 2007) is used, to focus on the precipitation anomalies associated with the ISO over the WNP. Our study period is from 1980 to 2018.

MSE is often used to reveal the dominant processes for the eastward propagation of boreal-winter MJO (Maloney 2009) and northward propagation of boreal-summer ISO (Jiang 2017; Wang and Li 2020). MSE is defined as the sum of sensible heat, latent heat, and potential energy, i.e., $m = c_p T + gz + Lq$, where T is temperature, z is height, and q is specific humidity. $c_p = 1004 \text{ J K}^{-1} \text{ kg}^{-1}$ is the specific

heat at constant pressure, $g = 9.8 \text{ m s}^{-2}$ is the gravitational acceleration, and $L = 2.5 \times 10^6 \text{ J kg}^{-1}$ is the latent heat of vaporization at 0°C . According to Maloney (2009), the column-integrated MSE budget can be calculated as follows:

$$\left\langle \frac{\partial m}{\partial t} \right\rangle = -\langle \vec{V} \cdot \nabla m \rangle - \left\langle \omega \frac{\partial m}{\partial p} \right\rangle + LH + SH + \langle LW \rangle + \langle SW \rangle$$

where \vec{V} is horizontal wind; ω is pressure velocity; p is pressure; LH and SH are latent and sensible heat fluxes at the surface, respectively; LW and SW are longwave and shortwave radiative heating rates, respectively. The angle brackets represent mass-weighted vertical integral from 1000 to 100 hPa. Specifically, $\langle LW \rangle$ and $\langle SW \rangle$ are defined as the difference between the top and surface radiative fluxes.

To select a longer period to cover most of the ISO signals, including the 12–25-day oscillation and 30–80-day boreal-summer ISO, a 12–80-day Butterworth band-pass filter is applied for all variables to extract the intraseasonal signals (Russell 2006). Note that the results are not sensitive to the selection of ISO range for filtering. Instead of studying WNP area-averaged OLR anomalies, we use the principal component (PC) of the dominant ISO mode over the WNP as the WNP ISO index, which is calculated by performing the Empirical Orthogonal Function (EOF) analysis on the boreal-summer intraseasonal OLR anomalies over the WNP. More details are given in Sect. 3. An ISO event over the WNP is defined when the WNP ISO index is above one standard deviation for three consecutive days. Using a different threshold does not change the results qualitatively. When two consecutive events happen within 12 days, we select the stronger one as one event and drop the smaller one because the ISO is supposed to have a period longer than 12 days. Day 0 is defined as the day when the WNP ISO index experiences its maximum for each ISO event. Because the ISO period mainly peaks within 60 days, the 61-day average with center on day 0 is selected to represent the background.

To identify the diversity of the ISO propagation, the K-means cluster, a centroid-based cluster method (Wilks 2011) widely used in atmospheric sciences (Wang et al. 2019a, b), is adopted here. In this method, the members are allocated to a specific number of clusters defined by their centroids; thus, the within-cluster sum of squares is minimized by repeating the process. After identifying individual ISO, the K-mean cluster is used to objectively classify the propagating patterns associated with the ISO over the WNP. Members for cluster analysis cover the spatial patterns of intraseasonal OLR anomalies on days -12 , -9 , -6 , -3 , and 0 over the Indo-Pacific region (40°E – 180° , 20°S – 40°N) for all selected ISO events. The silhouette value determines how similar an event is to its own cluster compared with the other clusters (Kaufman and Rousseeuw 2009), and a high silhouette value indicates that the member is well

matched to its own cluster and poorly matched to the neighboring clusters.

3 Dominant ISO mode over the WNP

During the boreal summer, the ISO usually prevails over the equatorial Indian Ocean, South Asian monsoon, and WNP regions when the Asian summer monsoon is formed (Fig. 1a), which is consistent with many previous observations (Lawrence and Webster 2002; Li and Wang 2005; Wang et al. 2009; Liu and Wang 2013). The ISO intensity over the WNP exhibits a robust seasonal cycle, with its peak from June to October (Fig. 1b). May, as a transitional month for the South China Sea monsoon onset (Kajikawa and Wang 2012; Wang et al. 2018), has lower ISO intensity than the months of June to October (JJASO) over the WNP. The ISO intensity over the WNP becomes stronger than those over the South Asian monsoon region and the equatorial Indian Ocean from June (not shown), and remains the strongest over the globe from June to October. Therefore, we define JJASO as the boreal summer for studying the ISO over the WNP. The region (110° – 140°E , 10° – 22.5°N) is defined as the WNP in this work, covering both the South China Sea (110° – 120°E , 10° – 22.5°N) and Philippine Sea (120° – 140°E , 10° – 22.5°N). The boreal-summer intraseasonal OLR anomalies averaged over the WNP show a broad and significant period from 12 to 60 days (Fig. 1c). Results from 5-day smoothing rather than band-pass filtering show similar results (not shown).

Most previous studies defined an WNP index as the area average of filtered OLR anomaly in a large domain (Hsu and Weng 2001; Liu et al. 2016; Wu and Cao 2017). Whether the ISO over the WNP is dominated by a uniform or a dipole mode across the South China Sea and Philippine Sea is not clear. We find that the ISOs averaged over the South China Sea and Philippine Sea are highly correlated, with a correlation coefficient of 0.53 ($p < 0.01$) from June to October during the whole study period of 1980–2018. To isolate the dominant intraseasonal signals in the whole WNP, we perform the EOF analysis on the intraseasonal OLR anomalies over the WNP during the boreal summer. The leading mode, explaining 36% of the total variance, shows uniform anomalies over the WNP (Fig. 2a). The precipitation associated with this leading mode shows similar results, except that the precipitation anomalies are maximum over the Philippine Sea and along the west coast of the Philippines, and the anomalies over the east part of the Philippines are relatively weak (Fig. 2b). The second and third modes exhibit northeast-southwest and northwest-southeast oriented dipole modes, respectively. This means that the peak phase of the dominant ISO mode over the WNP is in phase between the Philippine Sea and South China Sea. This leading mode

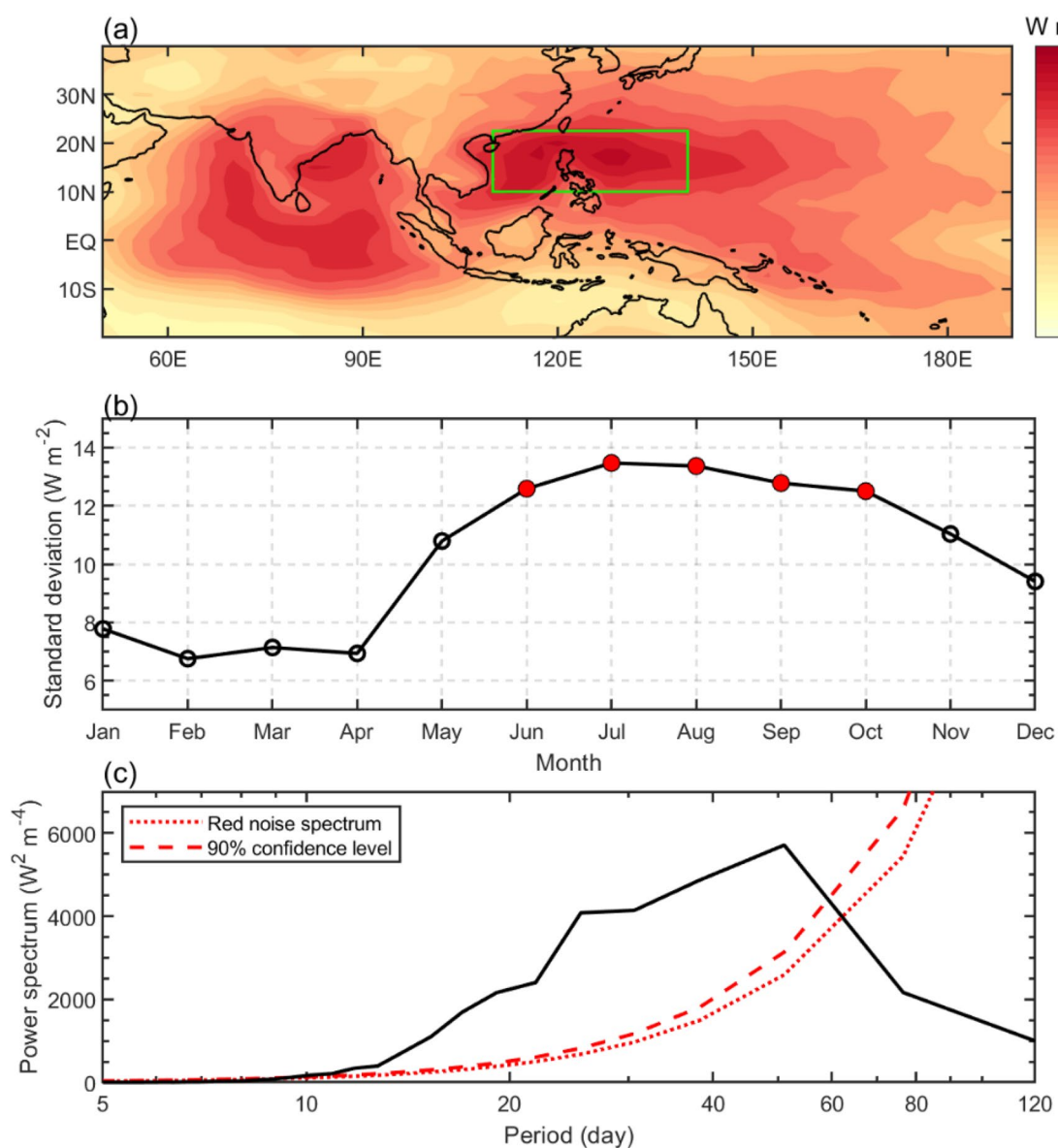


Fig. 1 Maximum intraseasonal oscillation (ISO) over the western North Pacific (WNP). **a** Standard deviation of intraseasonal OLR anomalies (W m^{-2}) during boreal summer from June to October over the tropical Indo-Pacific region. The intraseasonal signal is obtained by performing 12–80-day bandpass filtering. **b** Seasonal evolution of ISO intensity (W m^{-2}), represented by monthly standard deviation

of intraseasonal OLR anomalies over the WNP (110°–140° E, 10°–22.5° N). The red dots denote five maximum months. **c** Power spectrum ($\text{W}^2 \text{m}^{-4}$) of intraseasonal OLR anomalies averaged over the WNP during boreal summer from June to October. The red dotted and dashed lines denote red noise spectrum and 90% confidence level, respectively

is also highly correlated to the WNP area-averaged ISO. Therefore, we can use this PC as an index to represent the consistent ISO change over the WNP.

We use the PC of the leading ISO mode over the WNP as an index to select 139 ISO events based on the criteria given in Sect. 2. Similar results were obtained when using the WNP area-averaged intraseasonal OLR anomalies as the index (not shown). For all 139 ISO events, the ISO originates from the equatorial Indian Ocean on day –27, then

propagates northeastward, and forms a southeast–northwest tilted rain band spanning the Indian monsoon region to the MC on day –15 (Fig. 3), which is consistent with the canonical northeastward propagation of the boreal-summer ISO (Yasunari 1979; Annamalai and Sperber 2005; Liu et al. 2016). This tilted rain band, however, is very weak. The northwestward propagation over the western Pacific, found by many previous authors (Murakami 1984; Lau and Chan 1986; Nitta 1987; Chen and Murakami 1988; Wang and Rui

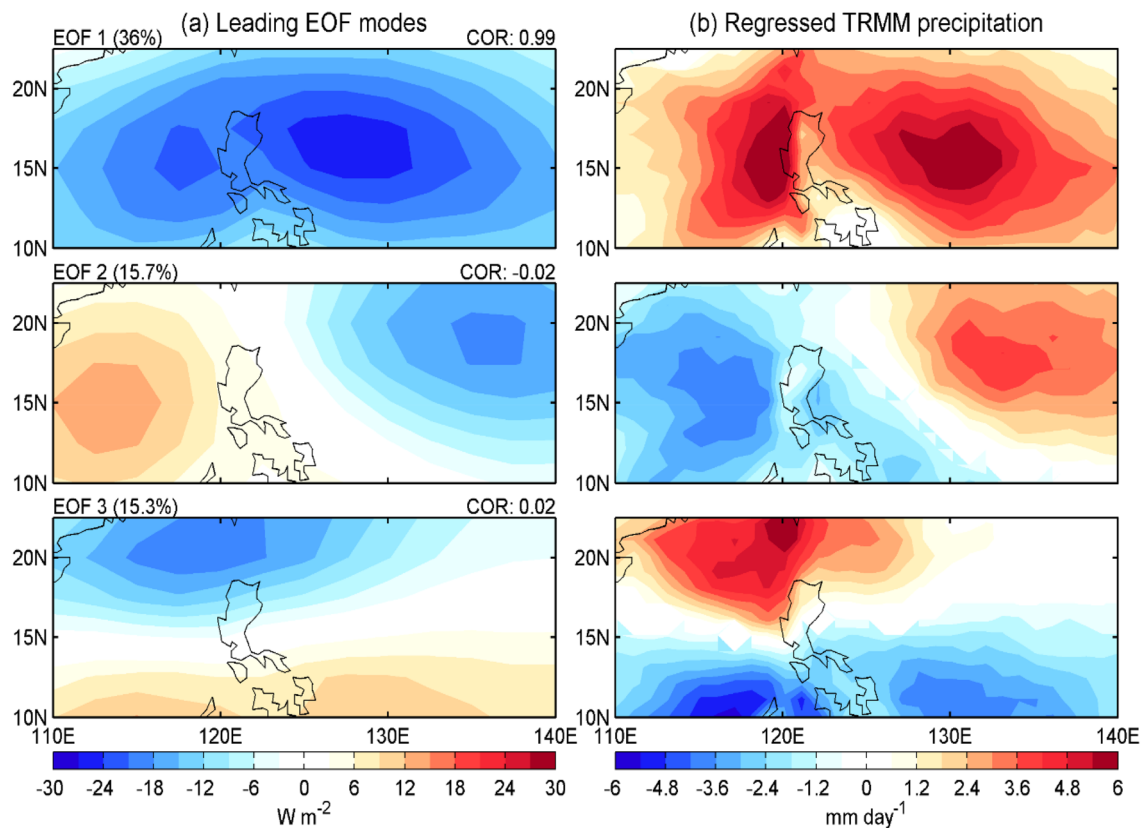


Fig. 2 Dominate mode of ISO over the WNP. **a** Three leading EOF modes of intraseasonal OLR anomalies over the WNP during boreal summer. Correlation coefficient with the WNP area-averaged intraseasonal OLR anomalies, multiplied by -1 , is given at the top right

corner of each panel. **b** Regressed intraseasonal TRMM precipitation anomalies according to the three leading EOF modes in (a). Shading shows significant signals at the 90% confidence level

1990; Hsu and Weng 2001; Kemball-Cook and Wang 2001; Yang et al. 2013), is observed since day -12 . These weak composited northeastward or northwestward propagations mean that the propagations associated with the ISOs over the WNP have greatly differences.

4 Diversity of ISO over the WNP

The K-mean cluster is applied to sorting out the propagation patterns of the WNP ISO, which are represented by the patterns of intraseasonal OLR anomalies on days -12 , -9 , -6 , -3 , and 0 over the Indo-Pacific region ($40^{\circ}E$ – 180° , $20^{\circ}S$ – $40^{\circ}N$) for all 139 selected ISO events. Sensitivity experiments showed that the results were not sensitive to the selection of the days used to represent the propagation of the ISO (not shown). The ISOs over the WNP can be objectively classified into three clusters of 41, 53, and 40 events, respectively. Classifications into more than three clusters will overproduce clusters that cannot be explained physically. Five events with negative silhouette values have been removed since they are poorly matched to their own clusters

(Kaufman and Rousseeuw 2009). Selection of different silhouette values does not change the composite characteristics of the three groups of ISOs (not shown), except for some associated background change.

The first cluster exhibits dominant westward propagation within the WNP (Fig. 4a). On day -12 when the dry ISO phase peaks over the WNP, a northeast-southwest tilted wave train extends from the WNP to the south of Japan. The cyclonic anomaly and wet ISO anomaly move southward to the Philippine Sea on day -6 . Then, this wet ISO anomaly extends westward to cover all the WNP region on day 0 . We call this group the westward cluster, in which the westward propagating wave train is normally related to the quasi-biweekly oscillation (Kikuchi and Wang 2009). Associated with this local oscillation within the WNP, a northward propagation of wet phase of ISO from the central equatorial Indian Ocean to South Asia is also observed.

The second cluster, which is called northeastward cluster, shows northeastward propagation from the equatorial Indian Ocean to the WNP (Fig. 4b), and is related to the canonical northeastward propagation of the boreal-summer ISO (Wang et al. 2009). The wet boreal-summer ISO,

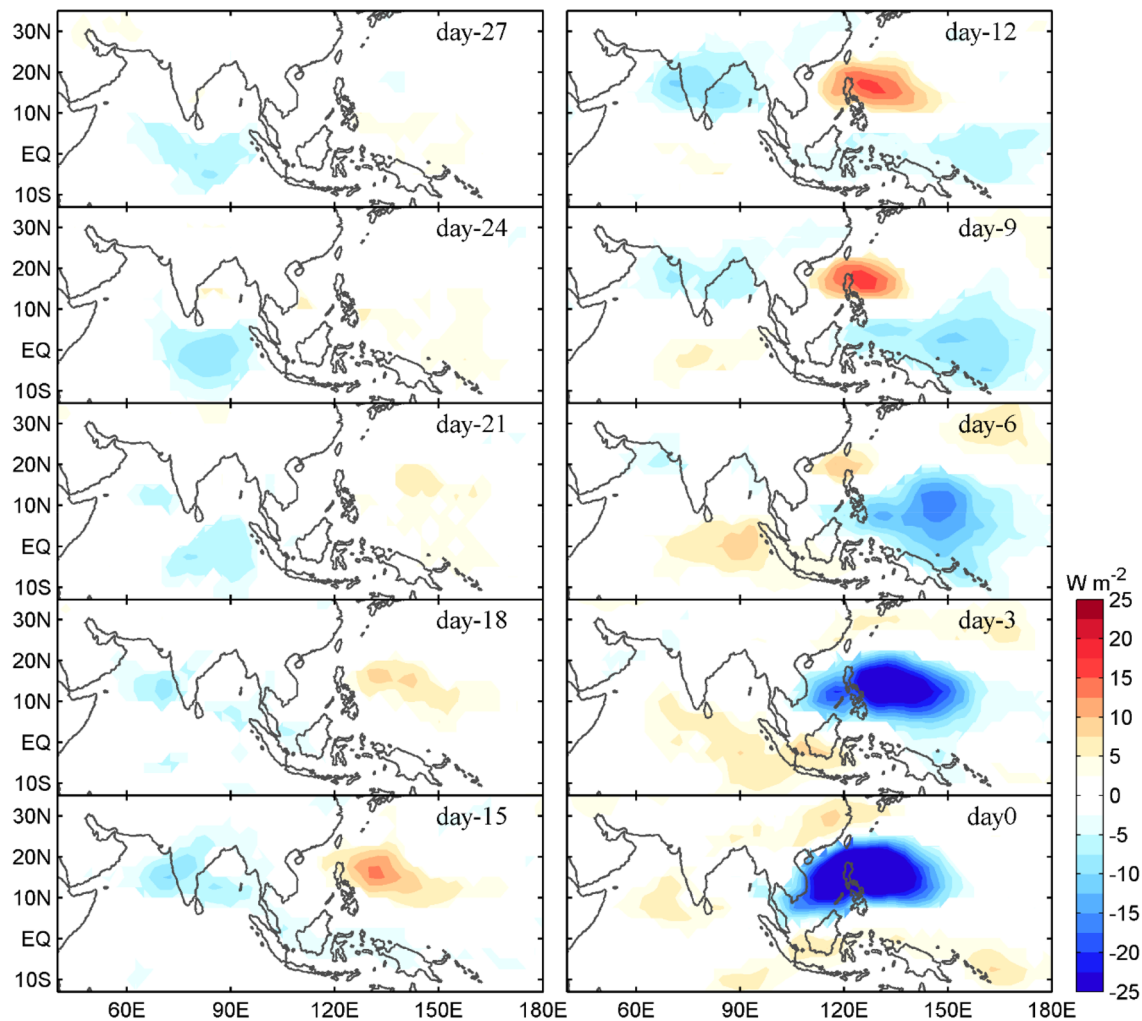


Fig. 3 Climatology and diversity of ISO over the WNP. Composite OLR intraseasonal anomalies (W m^{-2}) from day -27 to day 0 with interval of 3 days for all selected ISO events over the WNP. Shading shows significant signals at the 90% confidence level

initiated from the central equatorial Indian Ocean on day -27 (not shown), propagates northeastward and forms a northwest-southeast tilted rain band on day -12 across South Asia and the MC. This rain band can pass over the MC without being suppressed and move to the western Pacific; then, it propagates northward to the WNP, accompanied by strong cyclonic wind anomaly.

The third cluster, which is called northwestward cluster, exhibits northwestward propagation of a dipole structure across the Indian Ocean and western Pacific. This dipole is separated by the MC where no significant intraseasonal convection anomaly is observed (Fig. 4c). On day -12 , a zonal dipole structure with its dry phase over the WNP and its wet phase over South Asia is observed, accompanied by another dipole structure in the equator, with wet phase in the western Pacific and dry phase over the central Indian Ocean. This equatorial dipole structure then propagates northwestward and reaches South Asia and the WNP on

day 0 , followed by another out-of-phase dipole formed near the equator.

Our northeastward cluster is related to the simultaneous northward and eastward propagation defined by Pillai and Sahai (2015), which focused on the ISO originated from the central equatorial Indian Ocean. The Indian Ocean part of our northwestward cluster is partly related to the northward-only propagation in Pillai and Sahai (2015), while there is no significant signal over the Pacific related to their northward-only propagation over the Indian Ocean.

For these three clusters of ISOs over the WNP, the MSE anomalies also show westward, northeastward, and northwestward propagations. Their MSE anomalies coincide with the OLR anomalies very well (Fig. 5), which means that the MSE analysis is suitable for representing the propagation of the ISO over the WNP and for diagnosing its diversity.

The MSE budget analysis is carried out to understand the relative importance of the components of the MSE budget

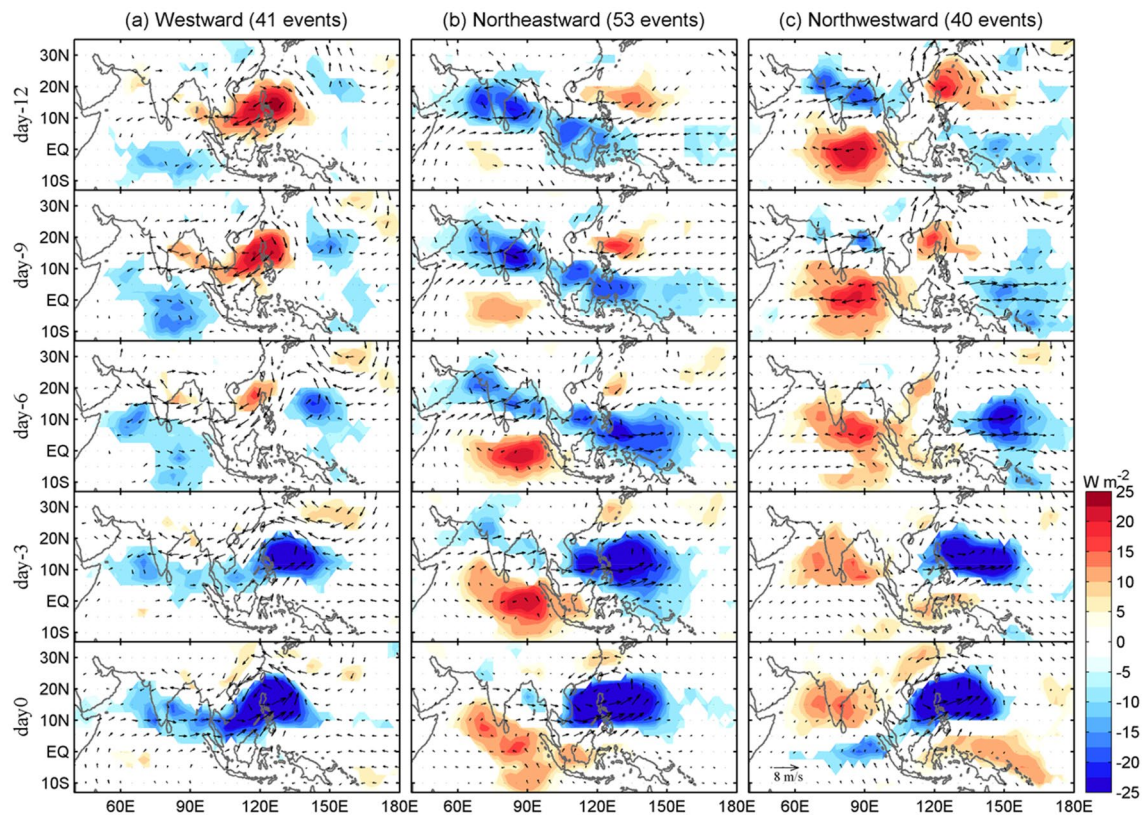


Fig. 4 Three types of ISO over the WNP. Composite intraseasonal OLR (W m^{-2}) and 850-hPa wind (m s^{-1}) anomalies from day -12 to day 0 during boreal summer for **a** westward, **b** northeastward, and

c northwestward clusters. Shading and vector indicate significant anomalies at the 90% confidence level

in different propagations of the three clusters. The positive MSE tendency anomaly in front of the convection, which favors the ISO propagation, is found in all three clusters (not shown). Let us take day -6 as an example (Fig. 6). The positive MSE tendency over the WNP is found in the west (Fig. 6a), northeast (Fig. 6b), and northwest (Fig. 6c) of the convective center for the three clusters, respectively. This positive MSE tendency for all three clusters is mainly contributed by horizontal advection. The vertical advection also has a positive feedback, but is very weak compared with the horizontal advection. The surface heat fluxes, including both latent and sensible heat fluxes, show negative anomalies over the WNP. The radiative heating rate is in phase with the convective center, maintaining the ISO rather than favoring its propagation. To sum up, the horizontal MSE advection contributes to these different propagations of the three clusters, which is consistent with previous findings on the boreal-summer ISO (Gonzalez and Jiang 2019; Wang and Li 2020). The radiative heating, however, provides an instability source for the ISO development.

We want to mention that this column-integrated MSE budget is not closed, especially over the Indian Ocean. This feature was mentioned in previous studies (Kiranmayi and

Maloney 2011; Kim et al. 2014), which can originate from the analysis increment in the model assimilation system (Kim et al. 2014).

5 Background-affected ISO diversity

Previous studies showed that the background mean state such as SST, humidity, and vertical shear can modulate the propagation of MJO and boreal-summer ISO (Liu et al. 2016; Wu and Cao 2017; Wang et al. 2019a; Wang and Li 2019). Figures 7 and 8 show composited background SST and column-integrated MSE anomalies as well as vertical wind shear of selected ISO events for the three clusters, where ISO events with higher silhouette values indicate larger similarity in their own groups. The background SST anomalies associated with the westward cluster depend on the selection of ISO cases with different similarities, and the positive SST anomalies over western Indian Ocean are more significant for the composite ISOs with larger similarity (Fig. 7a). The background eastern equatorial Pacific warming only occurs for those ISOs that are poorly matched with the westward propagation. The negative Pacific Meridional

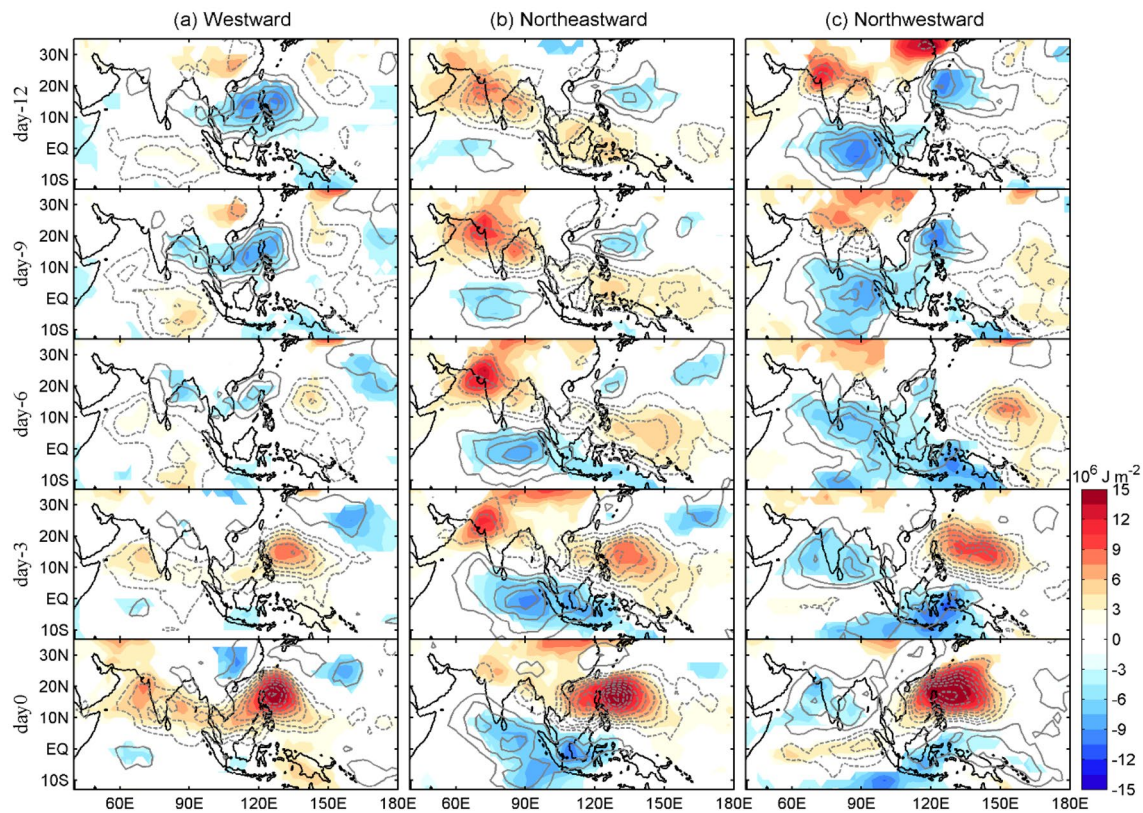


Fig. 5 Moist static energy (MSE) of three types of ISO over the WNP. Same as Fig. 4, except for MSE (J m^{-2}). Composite intra-seasonal OLR anomalies are shown by contours. Solid and dashed

contours indicate OLR anomalies great than 5 W m^{-2} and less than -5 W m^{-2} , respectively, with contour interval of 5 W m^{-2}

Mode (Chiang and Vimont 2004) and La Niña-like background are observed for the northeastward cluster, and the background anomalies are stable for the ISOs with different similarities (Fig. 7b). Note that even in the northeastward ISO events with large similarity, La Niña-like signals are not statistically significant, and the SST anomaly is mainly dominated by the negative Pacific Meridional Mode. The positive Pacific Meridional Mode is observed for the northwestward cluster, and the El Niño-like background only occurs for the ISOs with large similarity (Fig. 7c).

More significant background column-integrated MSE and vertical wind shear (defined by the difference between 200- and 850-hPa zonal winds) changes are also observed for the ISOs with larger similarity associated with these SST changes (Fig. 8). For the westward cluster (Fig. 8a), significant positive background MSE anomalies over the western Indian Ocean and negative or neutral background MSE anomalies around the MC show a clear indication of the westward background MSE gradient anomalies over the Indian Ocean as well as background westerly vertical shear anomalies. The eastward propagation of the MJO over the Indian Ocean is supposed to be suppressed by the westward gradient of background MSE anomalies and westerly

vertical shear anomalies (Adames and Kim 2016; Liu and Wang 2016; Jiang 2017). Therefore, no ISO originated from the Indian Ocean can pass over the MC and reach the WNP (Fig. 4a).

The weak positive background column-integrated MSE and associated easterly vertical shear anomalies over the western Pacific are confined near the equator (Fig. 8a), which cannot support the development of the ISO over the off-equatorial region before entering the monsoon trough. The negative background MSE anomalies over the WNP tend to weaken ISO amplitude, while it cannot prevent the ISO within the WNP because the mean MSE is $2.5 \times 10^7 \text{ J m}^{-2}$, which is much larger than the anomaly of $-1.3 \times 10^6 \text{ J m}^{-2}$ within the monsoon trough. Consequently, the ISO over the WNP is separated from the equatorial ISO and exhibits a local oscillation, which is dominated by the westward propagation within the WNP.

For the northeastward cluster, the background eastward MSE gradient anomaly from the Indian Ocean to the MC is observed (Fig. 8b), which is associated with the cold SST anomalies over the eastern equatorial Pacific and tropical North Pacific (Fig. 7b), favoring the eastward propagation of the ISO originated from the Indian Ocean (Adames and

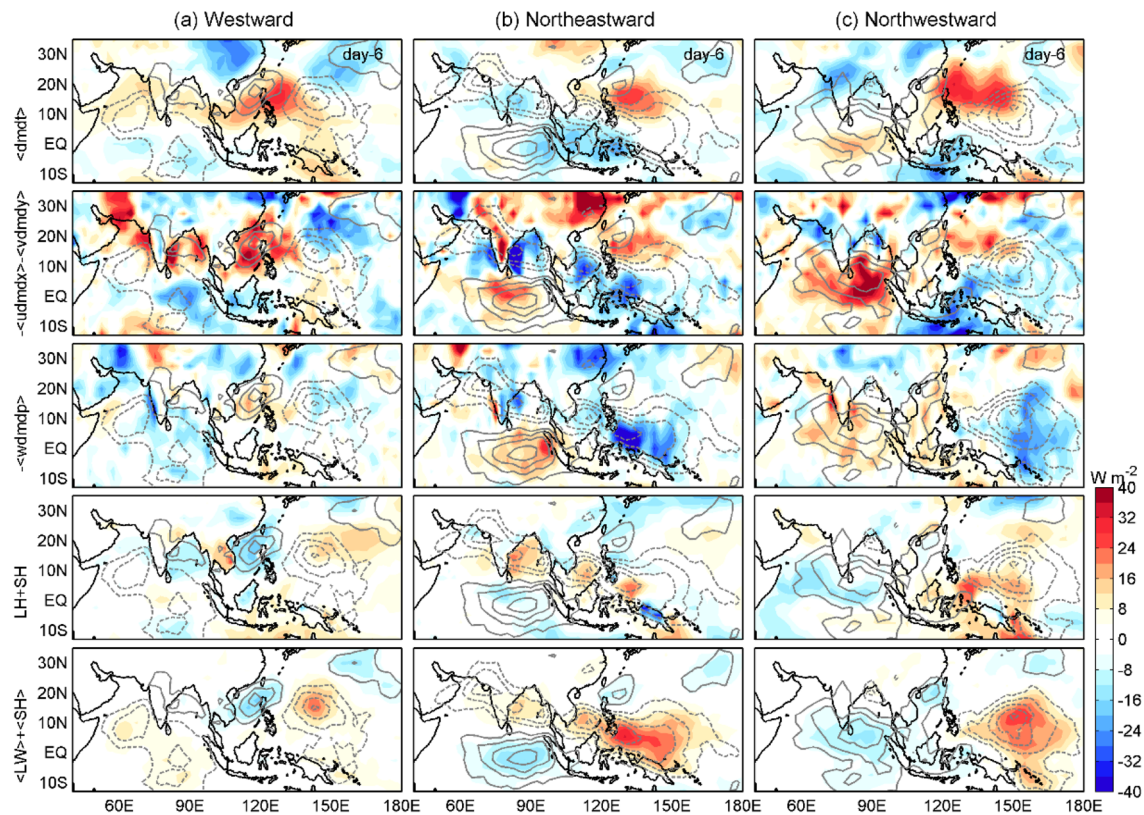


Fig. 6 MSE budget of three types of ISO over the WNP. Composite MSE budget terms (W m^{-2}) of MSE tendency, horizontal advection (meridional and zonal), vertical advection, surface heat fluxes (latent and sensible), and radiative heating rate (shortwave and longwave) at

day -6 for **a** westward, **b** northeastward, and **c** northwestward clusters. Solid and dashed contours indicate OLR anomalies greater than 5 W m^{-2} and less than -5 W m^{-2} , respectively, with contour interval of 5 W m^{-2}

Kim 2016; Liu and Wang 2016). Therefore, the ISO over the WNP is related to the northeastward propagation of the ISO originated from the Indian Ocean. The western Pacific is dominated by negative MSE and westerly vertical wind shear anomalies, resulting in suppressed ISO there (Fig. 4b).

For the northwestward cluster, different from the westward cluster whose background changes are only confined near the equator, strong positive MSE and easterly vertical wind shear anomalies over the western Pacific extend to 20°N (Fig. 8c), favoring the development and propagation of the ISO there. As a result, the ISOs, separated by the MC with negative background MSE anomaly, can prevail over the western Pacific and Indian Ocean through the local Walker circulation, forming a dipole structure (Fig. 4c).

The background changes include both annual cycle part and internal variability part from interannual to interdecadal time scales. The annual cycle is defined by the daily climatology for each calendar day. The internal variability part is calculated by performing composite on the anomalies with respect to the annual cycle (Fig. 9a, b). The annual cycle part is calculated by performing composite on the annual cycle, and the summer average is removed (Fig. 9c, d). For

those ISOs with large similarity, the background anomalies are mainly determined by the interannual-to-interdecadal variability for the northeastward and northwestward clusters, while the westward cluster is controlled by both the annual cycle and interannual-to-interdecadal variability.

6 Summary and discussion

The WNP ISO is the strongest from June to October, which has an important impact on the intraseasonal variability of the Asian summer monsoon system. We draw the conclusion that the leading mode of the ISO over the WNP exhibits in-phase anomalies between the South China Sea and Philippine Sea. The selected 139 WNP ISO events differ from each other in terms of their propagations, and can be classified into westward, northeastward, and northwestward clusters using the K-mean cluster analysis. The westward cluster is characterized by local westward propagation within the WNP, which is related to the quasi-biweekly oscillation. The northeastward cluster is related to the canonical propagation of the boreal-summer ISO originated from the equatorial

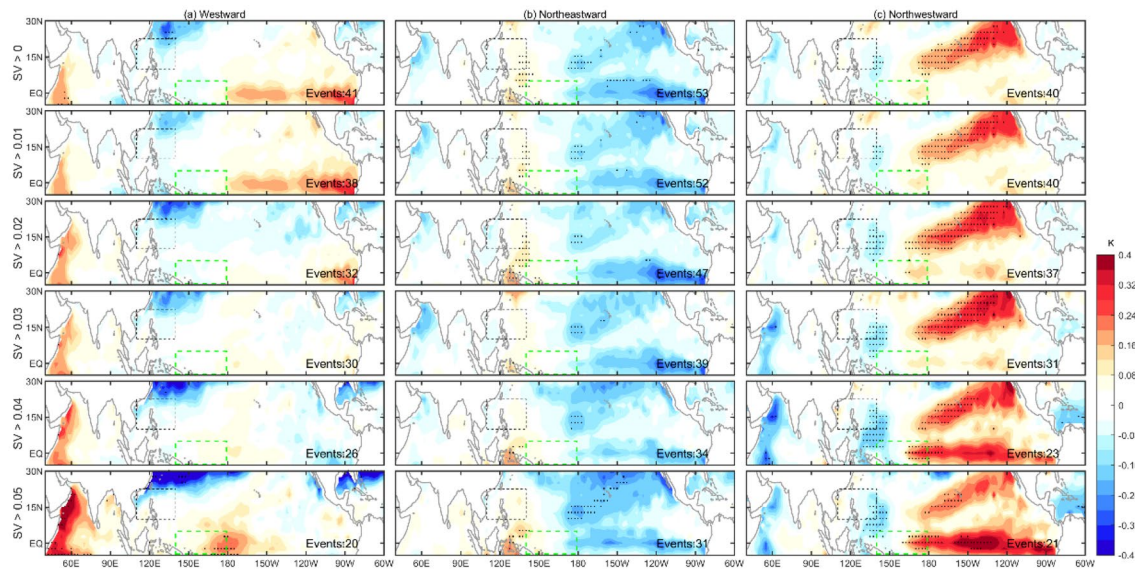


Fig. 7 Background SST changes associated with three types of ISO over the WNP. Background SST (K) are obtained by compositing the 61-day average of daily anomalies (derived from climatological boreal summer) with center on day 0 of selected ISO events with silhouette value (SV) larger than 0, 0.01, 0.02, 0.03, 0.04, and 0.05 for **a** westward, **b** northeastward, and **c** northwestward clus-

ters. The black and green boxes denote the WNP (110°–140° E, 10°–22.5° N) and western equatorial Pacific (140°–180° E, 5° S–5° N), respectively. Number at bottom right corner indicates the number of selected ISO events in each cluster. Stippling indicates significant anomalies at the 90% confidence level

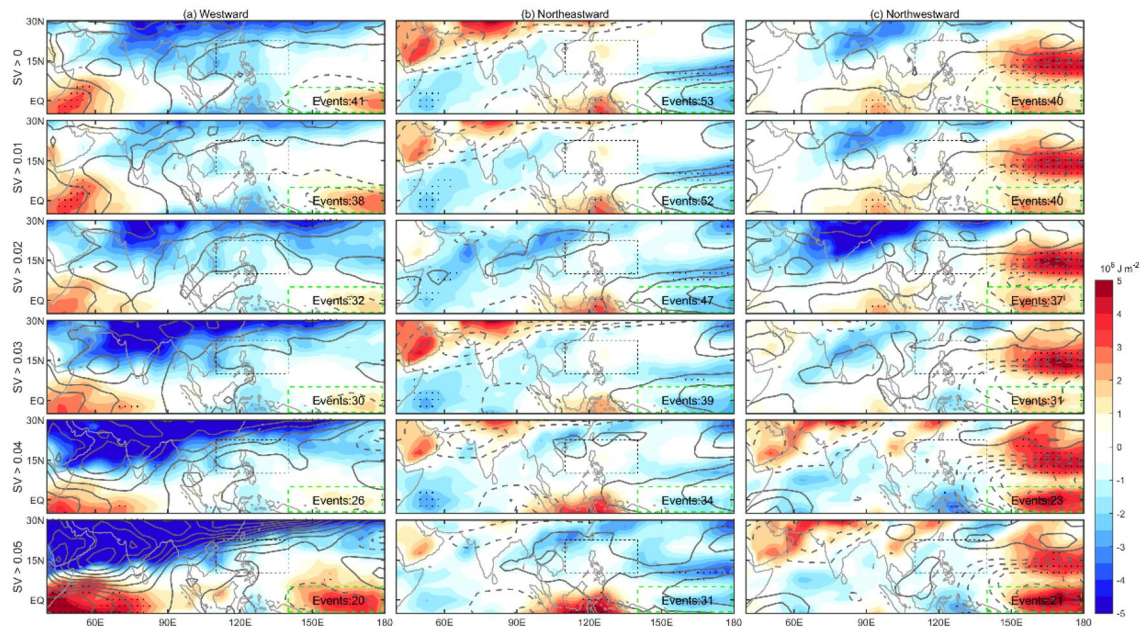


Fig. 8 Background MSE and vertical wind shear changes associated with three types of ISO over the WNP. Same as Fig. 7, but for vertically integrated MSE (shading; J m^{-2}) and vertical wind shear (con-

tour; m s^{-1}). Solid and dashed contours indicate vertical westerly and easterly wind shear anomalies, respectively, with contour interval of 10 m s^{-1}

Indian Ocean. The northwestward cluster, however, is denoted by a northwestward propagation of a dipole structure across the western Pacific and central Indian Ocean. The MSE exhibits divergent propagations associated with

these three clusters. The MSE tendency leading the ISO propagation is mainly contributed by horizontal advection, while radiative heating mainly works to maintain the ISO development.

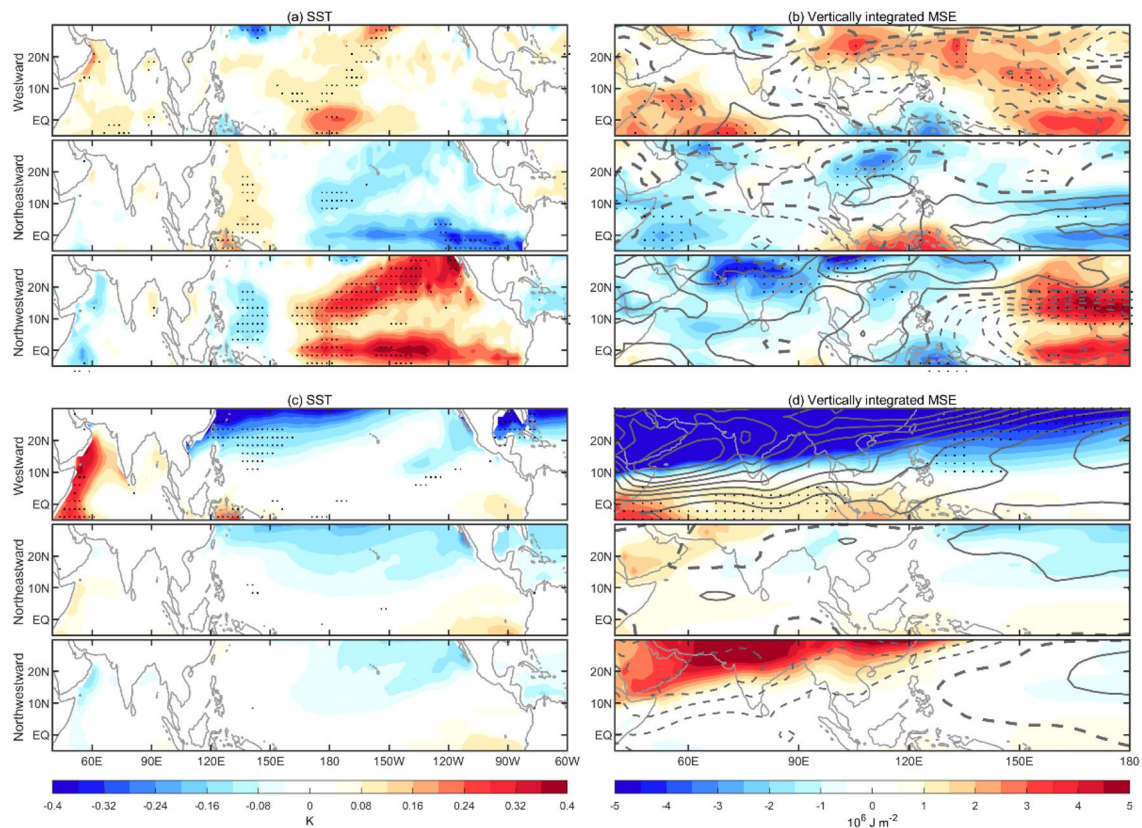


Fig. 9 Internal variability and seasonal cycle of mean state changes. Same as Figs. 7 and 8, except for **a, b** internal variability with anomalies derived from climatological annual cycle and for **c, d** climato-

logical annual cycle. Only ISO cases with silhouette value larger than 0.05 are composited

The three clusters are partly affected by the background changes, especially for those ISO events with large similarity, as summarized in Fig. 10. The westward cluster is related to a positive SST anomaly over the western Indian Ocean, and the westward gradient of background MSE anomaly prevents the eastward propagation of equatorial ISO (Fig. 10a). The northeastward cluster is enhanced by the eastward gradient of background MSE anomaly from the Indian Ocean to the MC associated with a negative Pacific Meridional Mode and La Niña-like background (Fig. 10b). The positive background MSE and easterly vertical wind shear anomalies over the western Pacific, associated with the positive Pacific Meridional Mode and El Niño-like pattern, enhance the western Pacific ISO, which couples with out-of-phase ISO over the Indian Ocean through a local Walker circulation to form a northwestward propagating dipole mode (Fig. 10c). These associated background changes mainly come from interannual-to-interdecadal variability for the latter two clusters, but come from both annual cycle and internal variability for the westward cluster.

Compared with the large background changes associated with the diversity of boreal-winter MJO (Wang et al. 2019a), the background changes associated with the

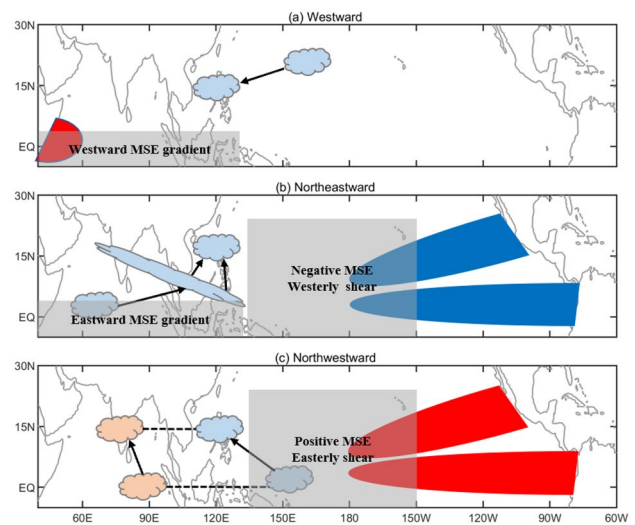


Fig. 10 Schematic diagrams for three types of ISO over the WNP. Shown are different ISO propagations and associated mean state changes for **a** westward, **b** northeastward, and **c** northwestward clusters. Clouds denote ISO convective center. Light blue and orange colors denote wet and dry phases of the ISO, respectively. Arrow denotes propagation of convection. Red shading denotes positive SST anomaly, and blue shading denotes the negative one. Rectangles are key regions with different changes of mean state

diversity of boreal-summer WNP ISO are relatively weak. This indicates the boreal-summer diversity is only partly determined by the background mean states, and atmospheric internal process also contributes to this diversity, challenging accurate prediction of the boreal-summer WNP ISO.

Due to the mean state-determined ISO diversity over the WNP, a new empirical subseasonal prediction system needs to consider these different types of mean states and associated diversity. A thorough investigation of whether our models can simulate this diversity of the ISO over the WNP should be carried out in the future, since our current simulations of boreal-summer ISO still face a big challenge (Lee et al. 2015; Neena et al. 2016; Jie et al. 2017).

Acknowledgements This work was supported by Guangdong Major Project of Basic and Applied Basic Research (2020B0301030004) and the Natural Science Foundation of China (41975107). BW acknowledges the support from the National Science Foundation of the U.S. (Award #2025057).

References

- Adames Á, Kim D (2016) The MJO as a dispersive, convectively coupled moisture wave: theory and observations. *J Atmos Sci* 73:913–941
- Annamalai H, Sperber KR (2005) Regional heat sources and the active and break phases of Boreal Summer Intraseasonal (30–50 Day) variability. *J Atmos Sci* 62:2726–2748
- Burleyson CD, Hagos SM, Feng Z, Kerns BWJ, Kim D (2018) Large-scale environmental characteristics of MJOs that strengthen and weaken over the maritime continent. *J Climate* 31:5731–5748
- Chen R, Wen Z, Lu R (2016) Evolution of the circulation anomalies and the quasi-biweekly oscillations associated with extreme heat events in Southern China. *J Climate* 29:6909–6921
- Chen TC, Chen JM (1995) An observational study of the South China Sea monsoon during the 1979 summer: onset and life cycle. *Mon Weather Rev* 123:2295–2318
- Chen TC, Murakami M (1988) The 30–50 day variation of convective activity over the Western Pacific Ocean with emphasis on the Northwestern Region. *Mon Weather Rev* 116:892–906
- Chiang J, Vimont D (2004) Analogous Pacific and Atlantic Meridional modes of tropical atmosphere–ocean variability. *J Climate* 17:4143–4158
- Dee DP et al (2011) The ERA-Interim reanalysis: configuration and performance of the data assimilation system. *Q J R Meteorol Soc* 137:553–597
- Deng L, Li T (2016) Relative roles of background moisture and vertical shear in regulating interannual variability of Boreal Summer intraseasonal oscillations. *J Climate* 29:7009–7025
- Fu J-X, Wang W, Ren H-L, Jia X, Shinoda T (2017) Three different downstream fates of the boreal-summer MJOs on their passages over the Maritime Continent. *Climate Dyn* 51:1841–1862
- Gonzalez AO, Jiang X (2019) Distinct propagation characteristics of intraseasonal variability over the tropical West Pacific. *J Geophys Res Atmos* 124:5332–5351
- Guan W, Hu H, Ren X, Yang X-Q (2019) Subseasonal zonal variability of the western Pacific subtropical high in summer: climate impacts and underlying mechanisms. *Climate Dyn* 53:3325–3344
- Hagos SM et al (2016) The impact of the diurnal cycle on the propagation of Madden-Julian Oscillation convection across the Maritime Continent. *J Adv Model Earth Syst* 8:1552–1564
- Hsu HH, Weng CH (2001) Northwestward propagation of the intraseasonal oscillation in the Western North Pacific during the Boreal Summer: structure and mechanism. *J Climate* 14:3834–3850
- Hsu P-C, Lee J-Y, Ha K-J (2016) Influence of boreal summer intraseasonal oscillation on rainfall extremes in southern China. *Int J Climatol* 36:1403–1412
- Hsu P-C, Lee J-Y, Ha K-J, Tsou C-H (2017) Influences of Boreal Summer Intraseasonal oscillation on heat waves in Monsoon Asia. *J Climate* 30:7191–7211
- Huang RH, Sun FY (1992) Impacts of the tropical western Pacific on the East Asian summer monsoon. *J Meteorol Soc Jpn* 70:243–256
- Huffman GA et al (2007) The TRMM multi-satellite precipitation analysis (TMPA): quasi-global, multiyear, combined-sensor precipitation estimates at fine scale. *J Hydrometeorol* 8:38–55
- Jiang X (2017) Key processes for the eastward propagation of the Madden-Julian Oscillation based on multimodel simulations. *J Geophys Res Atmos* 122:755–770
- Jie W, Vitart F, Wu T, Liu X (2017) Simulations of the Asian summer monsoon in the sub-seasonal to seasonal prediction project (S2S) database. *Q J R Meteorol Soc* 143:2282–2295
- Kajikawa Y, Wang B (2012) Interdecadal change of the South China Sea Summer Monsoon onset*. *J Climate* 25:3207–3218
- Kaufman L, Rousseeuw P (2009) Finding groups in data: an introduction to cluster analysis. Wiley, New Jersey. <https://doi.org/10.2307/2532178>
- Kemball-Cook S, Wang B (2001) Equatorial waves and air-sea interaction in the Boreal Summer intraseasonal oscillation. *J Climate* 14:2923–2942
- Kikuchi K, Wang B (2009) Global perspective of the quasi-biweekly oscillation. *J Climate* 22:1340–1359
- Kim D, Kug J-S, Sobel AH (2014) Propagating versus nonpropagating Madden-Julian oscillation events. *J Climate* 27:111–125
- Kiranmayi L, Maloney ED (2011) Intraseasonal moist static energy budget in reanalysis data. *J Geophys Res Atmos* 116
- Lau K-M, Chan PH (1986) Aspects of the 40–50 day oscillation during the Northern Summer as inferred from outgoing longwave radiation. *Mon Weather Rev* 114:1889–1909
- Lau WKM, Waliser DE, Hsu H-H (2012) Intraseasonal variability of the atmosphere–ocean–climate system: East Asian monsoon. Springer, Berlin. https://doi.org/10.1007/978-3-642-13914-7_3
- Lawrence DM, Webster PJ (2002) The Boreal Summer intraseasonal oscillation: relationship between northward and eastward movement of convection. *J Atmos Sci* 59:1593–1606
- Lee J-Y, Wang B, Wheeler MC, Fu X, Waliser DE, Kang I-S (2013) Real-time multivariate indices for the boreal summer intraseasonal oscillation over the Asian summer monsoon region. *Climate Dyn* 40:493–509
- Lee S-S, Wang B, Waliser DE, Neena JM, Lee J-Y (2015) Predictability and prediction skill of the boreal summer intraseasonal oscillation in the Intraseasonal Variability Hindcast Experiment. *Climate Dyn* 45:2123–2135
- Li RCY, Zhou W (2013) Modulation of Western North Pacific Tropical cyclone activity by the ISO. Part II: tracks and landfalls. *J Climate* 26:2919–2930
- Li T, Wang B (2005) A review on the Western North Pacific Monsoon: synoptic-to-interannual variabilities. *Terr Atmos Oceanic Sci* 16:285–314
- Li Y, Liu F, Hsu P-C (2020) Modulation of the intraseasonal variability of Pacific-Japan pattern by ENSO. *J Meteorol Res* 34:546–558
- Liebmann B (1996) Description of a complete (interpolated) outgoing longwave radiation dataset. *Bull Am Meteorol Soc* 77:1275–1277

- Linho, Wang B (2002) The time-space structure of the Asian-Pacific Summer Monsoon: a fast annual cycle view. *J Climate* 15:2001–2019
- Liu F, Li T, Wang H, Deng L, Zhang Y (2016) Modulation of Boreal Summer Intraseasonal Oscillations over the Western North Pacific by ENSO. *J Climate* 29:7189–7201
- Liu F, Wang B (2013) A mechanism for explaining the maximum intraseasonal oscillation center over the Western North Pacific*. *J Climate* 27:958–968
- Liu F, Wang B (2016) Role of horizontal advection of seasonal-mean moisture in the Madden-Julian Oscillation: a theoretical model analysis. *J Climate* 29:6277–6293
- Liu Y, Chan JCL, Mao J, Wu G (2002) The Role of Bay of Bengal convection in the onset of the 1998 South China Sea Summer Monsoon. *Mon Weather Rev* 130:2731–2744
- Liu F, Ouyang Y, Wang B, Yang J, Ling J, Hsu PC (2020) Seasonal evolution of the intraseasonal variability of China summer precipitation. *Clim Dyn* 54(11–12):4641–4655
- Maloney ED (2009) The moist static energy budget of a composite tropical intraseasonal oscillation in a climate model. *J Climate* 22:711–729
- Maloney ED, Hartmann DL (2000) Modulation of Eastern North Pacific Hurricanes by the Madden-Julian Oscillation. *J Climate* 13:1451–1460
- Maloney ED, Sobel AH (2004) Surface fluxes and ocean coupling in the tropical intraseasonal oscillation. *J Climate* 17:4368–4386
- Murakami M (1984) Analysis of the deep convective activity over the Western Pacific and Southeast Asia part II: seasonal and intraseasonal variations during Northern Summer. *J Meteorol Soc Jpn* 62:88–108
- Murakami T (1980) Empirical orthogonal function analysis of satellite-observed outgoing longwave radiation during summer. *Mon Weather Rev* 108:205–222
- Neena JM, Waliser D, Jiang X (2016) Model performance metrics and process diagnostics for boreal summer intraseasonal variability. *Climate Dyn* 48:1661–1683
- Nitta T (1987) Convective activities in the tropical western Pacific and their impact on the northern hemisphere summer circulation. *J Meteorol Soc Jpn* 65:373–390
- Pillai PA, Sahai AK (2015) Moisture dynamics of the northward and eastward propagating boreal summer intraseasonal oscillations: possible role of tropical Indo-west Pacific SST and circulation. *Climate Dyn* 47:1335–1350
- Raymond D (2001) A new model of the Madden-Julian oscillation. *J Atmos Sci* 58:2807–2819
- Ren X, Yang X-Q, Sun X (2013) Zonal oscillation of western Pacific subtropical high and subseasonal SST variations during Yangtze persistent heavy rainfall events. *J Climate* 26:8929–8946
- Russell DR (2006) Development of a time-domain, variable-period surface-wave magnitude measurement procedure for application at regional and teleseismic distances, part I: theory. *Bull Seismol Soc Am* 96:665
- Shao X, Huang P, Huang R-H (2014) Role of the phase transition of intraseasonal oscillation on the South China Sea summer monsoon onset. *Climate Dyn* 45:125–137
- Singh B, Kinter JL (2020) Tracking of tropical intraseasonal convective anomalies: I. Seasonality of the tropical intraseasonal oscillations. *J Geophys Res Atmos* 125
- Sobel A, Maloney E, Bellon G, Frierson D (2008) The role of surface fluxes in tropical intraseasonal oscillations. *Nat Geosci* 1:653–657
- Sun L, Wang H, Liu F (2019) Combined effect of the QBO and ENSO on the MJO. *Atmos Ocean Sci Lett* 12:170–176
- Sun X, Xu Y, Zhang Z, Yang X-Q (2019) The tropical and extratropical-origin summer meridional teleconnections over East Asia. *Climate Dyn* 53:721–735
- Tao SY, Chen LX (1987) A review of recent research on the East Asian Summer Monsoon in China. *Monsoon meteorology*. Oxford University Press, Oxford, pp 60–92
- Teng H, Wang B (2003) Interannual variations of the Boreal Summer Intraseasonal Oscillation in the Asian-Pacific Region. *J Climate* 16:3572–3584
- Wang B, Chen G, Liu F (2019) Diversity of the Madden-Julian Oscillation. *Sci Adv* 5:eaax0220
- Wang B, Huang F, Wu Z, Yang J, Fu X, Kikuchi K (2009) Multi-scale climate variability of the South China Sea monsoon: a review. *Dyn Atmos Oceans* 47:15–37
- Wang B et al (2019) Historical change of El Niño properties sheds light on future changes of extreme El Niño. *Proc Natl Acad Sci* 116:22512–22517
- Wang B, Rui H (1990) Synoptic climatology of transient tropical intraseasonal convection anomalies: 1975–1985. *Meteorol Atmos Phys* 44:43–61
- Wang H, Liu F, Wang B, Li T (2018) Effects of intraseasonal oscillation on South China Sea Summer monsoon onset. *Climate Dyn* 51:1–16
- Wang L, Li T (2019) Effect of vertical moist static energy advection on MJO eastward propagation: sensitivity to analysis domain. *Climate Dyn* 54:2029–2039
- Wang T, Li T (2020) Diagnosing the column-integrated moist static energy budget associated with the northward-propagating boreal summer intraseasonal oscillation. *Climate Dyn* 54:4711–4732
- Wheeler MC, Hendon HH (2004) An all-season real-time multivariate MJO index: development of an index for monitoring and prediction. *Mon Weather Rev* 132:1917–1932
- Wilks DS (2011) Statistical methods in the atmosphere science. Academic Press, San Diego
- Wu R, Cao X (2017) Relationship of boreal summer 10–20-day and 30–60-day intraseasonal oscillation intensity over the tropical western North Pacific to tropical Indo-Pacific SST. *Climate Dyn* 48:3529–3546
- Yang J, Bao Q, Wang B, Gong D-Y, He H, Gao M-N (2013) Distinct quasi-biweekly features of the subtropical East Asian monsoon during early and late summers. *Climate Dyn* 42:1469–1486
- Yasunari T (1979) Cloudiness fluctuations associated with the Northern Hemisphere Summer Monsoon. *J Meteorol Soc Jpn* 57:227–242
- Zhang C, Ling J (2017) Barrier effect of the Indo-Pacific Maritime Continent on the MJO: perspectives from tracking MJO precipitation. *J Climate* 30:3439–3459
- Zhao H, Jiang X, Wu L (2015) Modulation of Northwest Pacific Tropical cyclone genesis by the intraseasonal variability. *J Meteorol Soc Jpn* 93:81–97
- Zhou C, Li T (2010) Upscale feedback of tropical synoptic variability to intraseasonal oscillations through the nonlinear rectification of the surface latent heat flux. *J Climate* 23:5738–5754
- Zhou W, Chan JCL (2005) Intraseasonal oscillations and the South China Sea summer monsoon onset. *Int J Climatol* 25:1585–1609

Publisher's note Springer Nature remains neutral with regard to jurisdictional claims in published maps and institutional affiliations.